

# Multichannel image deblurring of raw color components

Mejdi Trimeche<sup>a</sup>, Dmitry Paliy<sup>b</sup>, Markku Vehvilainen<sup>a</sup>, Vladimir Katkovnik<sup>b</sup>

<sup>a</sup>Nokia Research Center, Tampere, Finland;

<sup>b</sup>Tampere University of Technology, Finland

## ABSTRACT

This paper presents a novel multi-channel image restoration algorithm. The main idea is to develop practical approaches to reduce optical blur from noisy observations produced by the sensor of a camera phone. An iterative deconvolution is applied separately to each color channel directly on the raw data. We use a modified iterative Landweber algorithm combined with an adaptive denoising technique. The adaptive denoising is based on local polynomial approximation (LPA) operating on data windows selected by the rule of intersection of confidence intervals (ICI). In order to avoid false coloring due to independent component filtering in the RGB space, we have integrated a novel saturation control mechanism that smoothly attenuates the high-pass filtering near saturated regions. It is shown by simulations that the proposed filtering is robust with respect to errors in point-spread function and approximated noise models. Experimental results show that the proposed processing technique produces significant improvement in perceived image resolution.

**Keywords:** deconvolution, iterative restoration, adaptive filtering, color processing, saturation control

## 1. INTRODUCTION

Image restoration research begun with the early space programs in the 1960s. Considering the cost and impact related to acquiring the images from space crafts, the degradation of the data was not a negligible problem. Hence, there was a critical need for processing techniques that could correct and revert the unwanted effects due to suboptimal systems, mechanical vibrations, motion, etc.<sup>1</sup> Although nowadays this approach towards image processing is still limited for high end applications, such as astronomy and medical imaging; its use in consumer electronics starts to take off, especially that more processing power is available in these devices, and that users are more aware of image quality on non-dedicated imaging platforms, such as camera phones.

Image restoration requires the knowledge of the degradation process in order to solve the consequent inverse problem. The inverse problem is generally ill-posed,<sup>2</sup> that is, if the direct solution is considered, a small perturbation in the input can result in an unbounded output. The direct inverse methods such as the regularized inverse (RI) and regularized wiener inverse (RWI) deconvolution techniques<sup>3</sup> are effective, but sensitive to modelling errors. On the other hand, the iterative methods are more robust<sup>4,5</sup>, hence, more interesting for practical implementations.

Several algorithms have been proposed to solve the ill-posed inverse problem by introducing a regularization step that suppresses over-amplification of the solution. For example, a directional adaptive regularization was proposed to reduce the ringing artifacts and the over-smoothing in the iterative restoration process.<sup>6</sup> Another regularization method<sup>7</sup> suggests the use of spatially adaptive intensity bounds in the framework of gradient projection method. The local bounds were shown to offer a flexible method for constraining the restoration problem. In this paper, we propose the use of a modified iterative Landweber algorithm which includes adaptive denoising filter. We used a method based on the local polynomial approximation (LPA), operating on windows that are selected by the rule of intersection of confidence intervals (ICI)<sup>8,9</sup>. This combination enhances the robustness of the iterative process towards the errors in the point-spread function (PSF) and in the noise parameters.

---

For further info, send correspondence to:

Mejdi Trimeche: mejdi.trimeche@nokia.com

Dmitriy Paliy: dmitriy.paliy@tut.fi

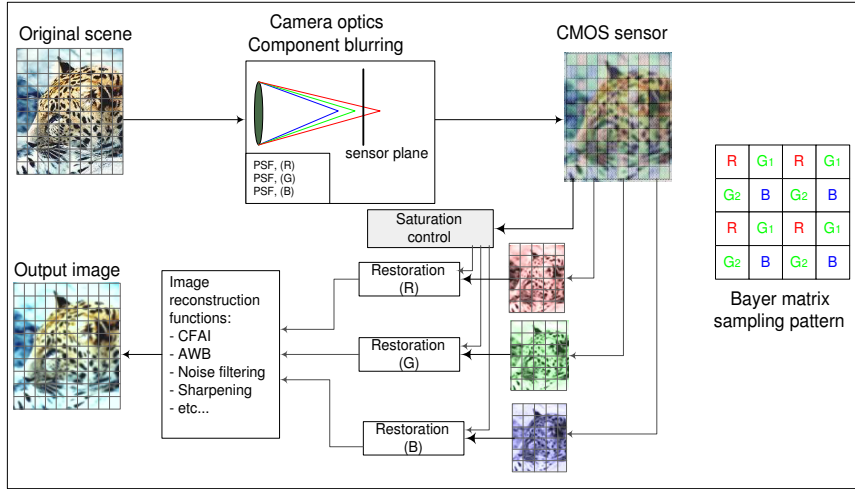


**Figure 1.** Block diagram of the proposed restoration system. The color channels are restored according to the corresponding component blur. The restoration algorithm is applied as the first operation in the image reconstruction chain in order to minimize non-linearities in the image formation model.

The specific problem of restoring noisy and blurred color images has been investigated in the literature since the mid-eighties. Several algorithms<sup>10,11,12</sup> have been proposed to restore the color images by utilizing the inter-channel correlation between the different color components. However, most of techniques approach the problem as a post-processing correction, that is, the processing is applied after the image is captured, processed, and stored. Our approach is inherently different. We consider the application of the image restoration algorithm directly (and separately) on the raw color image data, so that the deblurring and denoising are at the first step of the image reconstruction chain. Applying the image restoration as a pre-processing step ensures that the linear modelling of the problem holds best. Also, the choice of implementing the deblurring at this level of the image formation chain benefits the following cascaded operations from improved resolution and contrast. Example of the following typical processing steps include automatic white balance (AWB) and color filter array interpolation (CFAI) (typically non-linear operations). A similar processing paradigm was proposed earlier<sup>13</sup> in order to reduce color cross-talk and to decorrelate the different color components. However, the processing was carried out after color conversion, which may introduce the cross-talk itself. The restoration was proposed without consideration of the difference in the blur of the different color channels. In our work, we use separate processing of the raw RGB color components measured by the camera sensor, and we restore separately each channel according to the estimated optical blur. In fact, the optical blur in each color channel is different, since the focal length depends on the wavelength of the incoming light.<sup>14</sup>

In Section 2, we present the proposed processing paradigm and we describe the image acquisition model. In Section 3, the Landweber iterative restoration technique is briefly described and we introduce the modified iterative solution which includes the adaptive denoising technique. Analysis and simulation of the proposed deconvolution technique are also presented. In Section 4, we discuss the practical issues relating to the efficient implementation of the deconvolution algorithm. Finally, experimental results with the proposed technique on images taken with a fixed-focus camera are shown.

## 2. RESTORATION AS A PRE-PROCESSING STEP

Fig. 1 depicts the block diagram of the proposed multi-channel restoration within the image reconstruction chain. In the model we consider, the incoming light is blurred by the camera optics, and the image data is measured by a sensor through the Bayer sampling pattern. The optical blurring and the noise sensitivity of each color channel can be different. In fact, by implementing the restoration directly on the raw color components,

we are aiming to avoid nonlinearities produced by the cascaded image reconstruction functions like AWB, CFAI, sharpening,<sup>15</sup> etc...

If we assume a linear response at the sensor and a linear space-invariant blur in each color channel, then the observed image can be modelled as:

$$z_i(x) = (v_i * y_i)(x) + \eta_i(x), \quad i = 1, \dots, 4 \quad (1)$$

where  $z_i$  is the measured color component image,  $y_i$  is the original color component,  $v_i$  is the corresponding PSF in that component, and  $\eta_i$  is an i.i.d. additive Gaussian noise term.  $z_i$ ,  $y_i$  and  $\eta_i$  are defined over the array  $x = (m, n)$  of pixels spanning the entire image area. In equation (1), " $*$ " is the discrete convolution operator. The index  $i = \{1, 2, 3, 4\}$  denotes respectively the data corresponding to the *Red*, *Green1*, *Green2*, and *Blue* color channels, those are measured according to the Bayer matrix sampling pattern. Note that each of these images is quarter size of the final output image. The restoration problem can be stated as recovering the original image  $y_i$  from its degraded observation  $z_i$ .

### 3. RESTORATION METHODS

#### 3.1. Generalized Landweber method with filtering

Iterative methods have shown to be an attractive alternative for implementing the inverse solution of image deblurring, especially when the blurring parameters can exhibit some modelling errors. The standard *Landweber method*<sup>4,16</sup> to solve for  $y_i$  from the observations  $z_i$  in equation (1) is given by the following iterative process:

$$\begin{aligned} y_i^{(0)} &= 0, \\ y_i^{(k+1)} &= y_i^{(k)} + \mu_i \cdot v_i^T * (z_i - v_i * y_i^{(k)}), \quad k = 0, 1, \dots, \quad i = 1, \dots, 4, \end{aligned} \quad (2)$$

where  $\mu_i$  is the update parameter,  $v_i^T(t) = v_i(-t)$ . If the image formation model (1) is noise-free,  $\eta_i(t) = 0$ , the iterative process described above is converging.<sup>16</sup> However, the slow convergence<sup>4</sup> is a significant drawback. The problem of choosing  $\mu_i$  is one of balancing the stability against the rate of convergence, i.e., a large  $\mu_i$  ensures a quick convergence but also increases a risk of instability.

Another aspect of the Landweber method in equation (3) is the fact that it is designed to solve a problem  $z_i(t) = (v_i * y_i)(t)$ . As a result, the obtained solution is sub-optimal in presence of noise. We propose to use the following modifications in order to incorporate a noise filtering stage and to enhance convergence:

$$\begin{aligned} y_i^{(0)} &= 0, \\ y_i^{(k+1)} &= \tilde{y}_i^{(k)} + \mu_i \cdot d_i * v_i^T * (z_i - v_i * \tilde{y}_i^{(k)}), \\ \tilde{y}_i^{(k+1)} &= \Phi\{y_i^{(k+1)}\}, \quad k = 0, 1, \dots, \quad i = 1, \dots, 4 \end{aligned} \quad (4)$$

where  $d_i$  is an impulse response of a special linear filter that can be used to accelerate the *convergence* of the solution.  $\Phi\{\cdot\}$  is an intermediate filtering operator that is intended to enhance the robustness of the solution. It can be considered as a separate regularization step. It is interesting to note that in the context of *expectation-maximization* (EM) methods,<sup>17</sup> in the iterative process described above, the E-step coincides with equation (5), and M-step corresponds to filtering stage in equation (6).

The operator  $\Phi\{\cdot\}$  can be, for example, a simple averaging filter, or any other sophisticated filter that takes into consideration the local signal statistics. In this paper, we chose to plug-in an adaptive denoising filter in order to preserve the image details from over-smoothing. The adaptive filter is based on the polynomial approximation of neighboring pixels from dynamically selected windows. The windows are selected by the rule of intersection of confidence intervals in order to ensure statistical homogeneity of the data in the localized windows. Detailed explanation and results of this filtering approach (LPA-ICI) can be found in the following references<sup>8,9</sup>. This adaptive denoising technique plays an important role in our proposed solution because it preserves image details and ensures also efficient noise removal, which is difficult to achieve using filters operating on fixed data support.

### 3.2. Convergence

To study the convergence and the sensitivity of the proposed iterative deconvolution technique, we carry out the analysis in the Fourier domain. The image formation model in equation (1) can be written in the frequency domain as follows:

$$Z_i(\omega) = V_i(\omega)Y_i(\omega) + \eta_i(\omega), \quad i = 1, \dots, 4 \quad (7)$$

where  $Y_i(\omega) = \mathcal{F}\{y_i(x)\}$  is the Fourier transform of  $y_i$ ,  $Z_i(\omega) = \mathcal{F}\{z_i(x)\}$ ,  $V_i(\omega) = \mathcal{F}\{v_i(x)\}$ , and  $\eta_i(\omega) = \mathcal{F}\{\eta_i(x)\}$ .

Now, consider the equations (4-5) in the frequency domain:

$$\begin{aligned} Y_i^{(0)} &= 0, \\ Y_i^{(k+1)} &= Y_i^{(k)} + \mu_i D_i V_i^* (Z_i - V_i Y_i^{(k)}), \quad k = 0, 1, \dots, \quad i = 1, \dots, 4 \end{aligned} \quad (8)$$

where,  $D_i(\omega) = \mathcal{F}\{d_i(x)\}$ , and  $V_i^*$  is the complex conjugate of  $V_i$ . If we rewrite Eq. (8) in the following form:

$$Y_i^{(k+1)} = Y_i^{(k)} + \mu_i D_i V_i^* (Z_i - V_i Y_i^{(k)}) = (1 - \mu_i D_i |V_i|^2) Y_i^{(k)} + \mu_i D_i V_i^* Z_i, \quad (9)$$

then the error between the original signal and the signal estimate in the frequency domain can be expressed as:

$$E_i^{(k+1)} = q_i E_i^{(k)} - \mu_i D_i V_i^* \eta_i, \quad q_i = 1 - \mu_i D_i |V_i|^2, \quad (10)$$

where  $E_i^{(k)} = \mathcal{F}\{e_i^{(k)}\}$ ,  $e_i^{(k)} = y_i - y_i^{(k)}$ .

The idea behind using the operator  $D_i$  is to accelerate the iterative process (8), while at the same time ensure that the overall solution converges. As it can be inferred from equation (10), the rate of convergence of the iterative process (8) is characterized by the variable  $q_i(\omega) = 1 - \mu_i D_i(\omega) |V_i(\omega)|^2$ . Further, the convergence takes a place only if  $|q_i(\omega)| < 1$ . This gives us the conditions that the update parameter  $\mu_i$  has to satisfy:

$$0 < \mu_i D_i(\omega) |V_i(\omega)|^2 < 2, \quad \text{for all } \omega, \quad (11)$$

where it is assumed that  $D_i(\omega)$  is real and positive everywhere on its frequency support. Note that for the pure Landweber method in equation (3),  $D_i = 1$ .

The fastest convergence happens when factor  $q_i$  (10) is minimal. If we introduce the following variable:

$$\lambda_{i,\max} = \max_{\omega} D_i(\omega) |V_i(\omega)|^2, \quad (12)$$

then, according to equation (11), we can ensure convergence of the solution by selecting  $\mu_i$  as follows:

$$\hat{\mu}_i = \frac{2}{\lambda_{i,\max} + \epsilon}, \quad (13)$$

where  $\epsilon > 0$ . When considering frequency domain implementations of the iterative process in (8), we propose to use the following realization of  $D_i$  in order to accelerate convergence:

$$D_i = \frac{1}{|V_i|^2 + r_i^2}, \quad (14)$$

where  $r_i^2$  is a regularization parameter. This can be motivated by the fact that this choice of  $D_i$  allows us to approach the behavior of the pseudo-inverse filter at each iteration. This allows us to accelerate significantly the solution. In fact, it can be seen from equation (9), that the pseudo-inverse filter can be a particular case of this realization when  $\mu_i = 1$ .

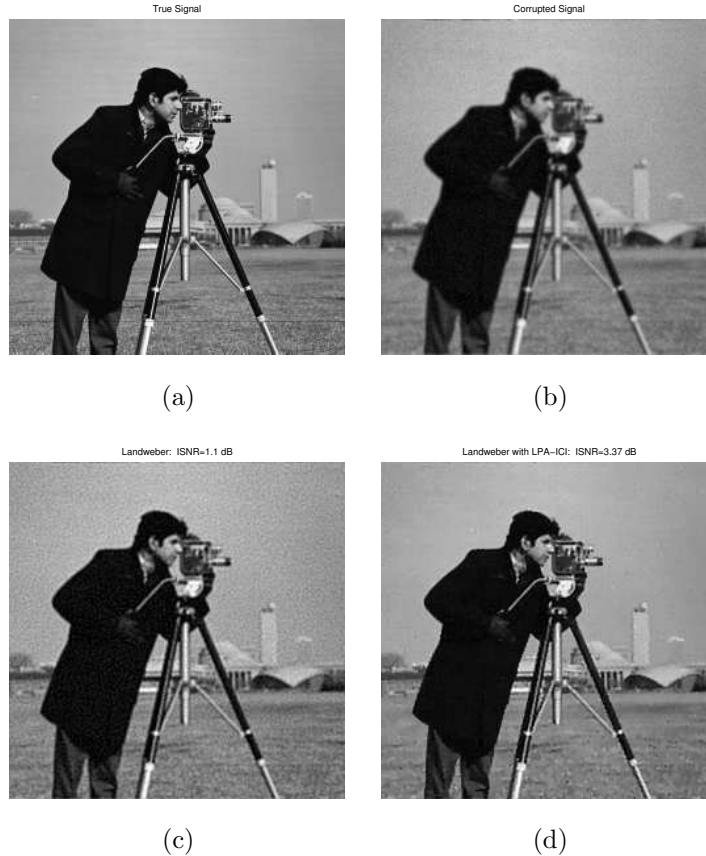


**Figure 2.** (a) Original *Cameraman* test image (b) blurred and noisy image, Gaussian PSF  $\sigma_{blur} = 1$ . Gaussian additive noise,  $\sigma_{noise}^2 = 0.02$ . (c) Restoration result with the standard iterative Landweber method after 7 iterations. (d) Proposed Landweber method with *LPA – ICI* after 4 iterations.

### 3.3. Simulation results with LPA-ICI regularization

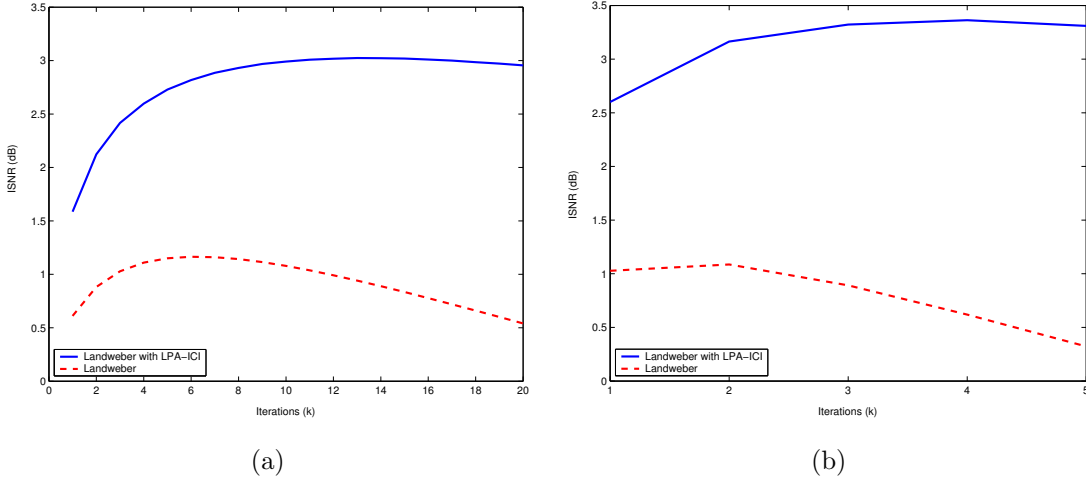
For studying properties of the proposed method we used the *Cameraman* test image (Fig.2a) which was corrupted by a Gaussian PSF blur:

$$v_{\sigma_{blur}}(m, n) = \frac{1}{2\pi\sigma_{blur}^2} \exp\left(-\frac{m^2 + n^2}{2\sigma_{blur}^2}\right). \quad (15)$$

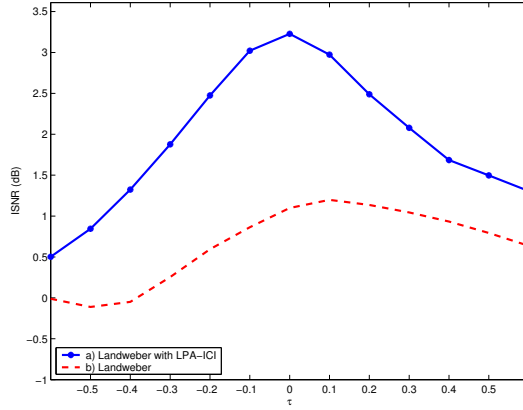
We used  $\sigma_{blur}^2 = 1$ . We further degraded the blurred image with an additive white Gaussian noise,  $\sigma_{noise}^2 = 0.02$  (Fig.2b). We compared the restoration results obtained with the standard Landweber method (Fig.2c) against the proposed method with the integrated LPA-ICI filtering (Fig.2d). It can be seen from the images and from the improvement in signal to noise ratio (ISNR) values that the proposed denoising step significantly enhances the performance of the restoration process. It is worth mentioning that the images shown above correspond to the results of the implementation in frequency domain.

Fig.3a shows the improvement in terms of SNR across the iterations for the restored images in Fig.2c and Fig.2d. The ISNR corresponding to the standard Landweber technique (dashed line) takes its maximum and then tends down, due to the noise amplification. The curve corresponding to the proposed technique with LPA-ICI denoising (solid line) clearly improves the stability of the solution. In fact, this adaptive filtering stage acts as a regularization for the inverse solution, while also enhancing the overall quality of restored images.

In Fig. 3b, we integrated the acceleration operator  $D_i$  in equation (14) into the frequency domain implementation of the iterative restoration. It can be seen that the number of iterations that is needed to achieve similar



**Figure 3.** ISNR ( $dB$ ) vs. number of iterations ( $k$ ). (a) Iterative methods *without* acceleration. (b) Iterative methods *with* acceleration. In both figures we compared Landweber technique with LPA-ICI denoising (*solid line*) and the standard Landweber technique without denoising (*dashed line*).



**Figure 4.** Simulation of the sensitivity of the iterative deblurring methods to possible errors in PSF estimates ( $\hat{v}_i$ ). We used Gaussian PSF with parameter  $\sigma_{blur} = 1 \pm \tau$ , where  $\tau$  is an error that is deliberately introduced .

performance is significantly smaller. This result confirms the potential of integrating an accelerating spatial operator in the Landweber process in general.

### 3.4. Sensitivity to PSF errors

In practice, it is rarely possible to have precise estimates for the point spread function (PSF). Therefore, it is essential to have restoration algorithms that are robust against deviations in PSF.

In order to test the robustness of the proposed solution, we run the algorithms when the exact PSF  $v_i$  is known, and when we deliberately introduced different amounts of errors  $\Delta v_i$  into the input PSF to the restoration algorithms ( $\hat{v}_i$ ). The corrupted PSF that is actually used in the restoration model can be expressed as follows:

$$\hat{v}_i = v_i + \Delta v_i, \quad i = 1, \dots, 4. \quad (16)$$

In our experiments, we used Gaussian PSF  $\hat{v}_i$  with parameter  $\sigma_{blur} = 1 \pm \tau$ , where  $\tau \in \{0, 0.1, \dots, 0.6\}$  is the assumed estimation error. In Fig. 4, we compared the proposed technique (solid line) with the standard

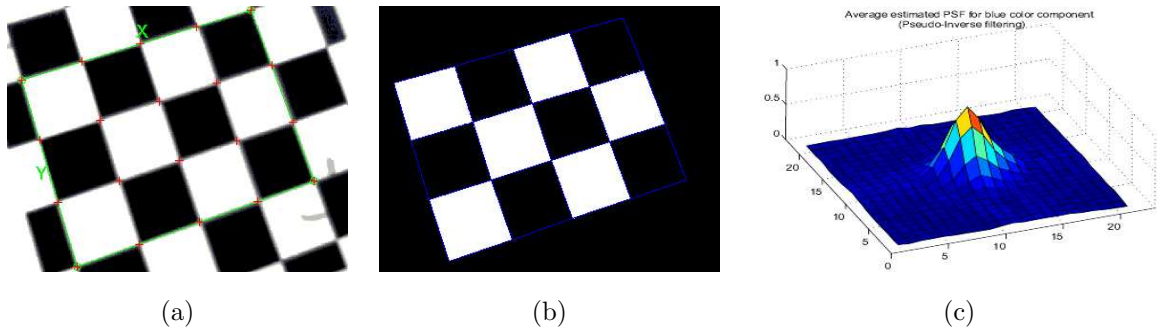


**Figure 5.** Procedure to estimate the PSF. (a) From the captured raw image corresponding to each color channel; the corners of the checker-board are located at sub-pixel accuracy. (b) The corner locations are used to reconstruct the sharp pattern of the original checkerboard images. (c) An example of the estimated PSF for the blue color channel using raw data from Nokia 6600 camera phone. 10 images are used in the calibration process, all were captured at close range ( $\sim 10\text{cm}$ ).

Landweber method (dashed line). It is clear from the ISNR curves that the proposed solution is more robust against possible errors in PSF, since the performance was consistently better than the standard Landweber method for all the values of  $\tau$  that were used.

## 4. PRACTICAL CONSIDERATIONS

### 4.1. Blur identification

Typically, one of the most difficult practical problem to be solved when restoring images is usually not the choice of a restoration algorithm itself, but rather finding a good PSF. The problem is that the PSF changes as a function of the wavelength and the distance of the imaged target with respect to the camera. In this paper, we simplify the problem by assuming out-of-focus close range imaging. We further assume space invariant blurring. In order to enable the application of the restoration algorithms to the images of a camera phone, we have developed a simple PSF estimation technique, and used it to find the blurring corresponding to each color component. The procedure is described next.

Given a blurred raw image corresponding to one color component of a checker-board pattern, the four outer corner points are located manually, and a first rough estimate of the corner positions is calculated. Next, the exact locations (at sub-pixel accuracy) are recalculated again by refining the search within a square window of  $10 \times 10$  pixels. The algorithms for corner detection are based on the implementation of the OpenCV<sup>18</sup> calibration toolbox. Using those corner points, we reconstruct an approximation for the original grid image by averaging the central parts of each square and by asserting a constant luminance value to those squares. Fig.5a shows an example of a test image, and Fig.5b shows the corresponding segmented and reconstructed grid image. Now that we obtained the blurred image (Fig.5a), and the assumed original input (Fig.5b), the blur can be inferred by applying an inverse filtering method.

In our experiments, we used simple pseudo-inverse filtering (in Fourier domain) to obtain the PSF estimates. Since the pseudo-inverse technique is quite sensitive to noise, we further imposed a low pass cut-off frequency to limit the noise propagation. We repeated the procedure with several images (more than 10, with different orientations of the checkerboard images), and we finally averaged all of them to obtain smooth and reliable estimates. Fig.5c shows an example of the estimated PSF for the blue color channel with a truncated support of  $21 \times 21$  pixels. In our experiments, it was also confirmed that the 3 color components exhibited slightly different blurring characteristics, interestingly, the blue color component, although it was least contrasted, was the sharpest component.

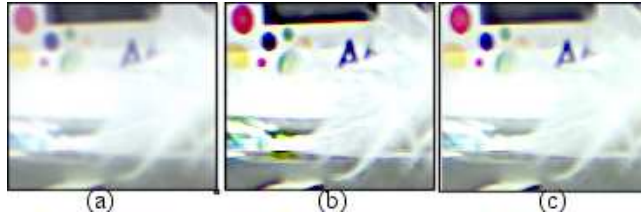


**Figure 6.** Effect of the proposed saturation control mechanism to avoid false coloring in restored images. (a) Original blurred image (b) Restored image (4 iterations) without saturation control, remark the green false coloring. (c) Restored image (4 iterations) with saturation control. The green false coloring has disappeared. Same reconstruction chain used in all 3 images.

## 4.2. Implementation of restoration

In order to realize practical real time implementations of the restoration algorithm in equations (4-6), some approximations in the algorithm have been considered. We have implemented a simplified integer implementation of the algorithm. This causes a loss of precision in the normalized PSF. Because the linear convolution is proportional to the square of the size of the filter support, we have truncated the PSF support to a window of 9x9, which contains most of the information about the defocus degradation. We considered also a fast implementation of an approximation to the formal solution in equation (4-6). We assume that the first approximation in (4) is the observed image itself. So, the iterative approximate solution can be compactly expressed as:

$$y_i^{(0)} = z_i, \quad (17)$$

$$y_i^{(k+1)} = \tilde{y}_i^{(k)} + \mu_{i,adap} \cdot \tilde{v}_i * (z_i - v_i * \tilde{y}_i^{(k)}), \quad (18)$$

$$\tilde{y}_i^{(k+1)} = \Phi\{y_i^{(k+1)}\}, \quad i = 1, \dots, 4 \quad (19)$$

where  $\mu_{i,adap}$  is a pixel-wise step size parameter that is designed to avoid false coloring. It is derived in the following section.

## 4.3. Saturation control

In the literature, the formulation of the image acquisition process is invariably assumed to be a linear one (equation 1). It is true that this assumption simplifies the inverse problem and allows to develop compact and attractive solutions. However, in practice, the sensor electronics introduce nonlinearities in the acquisition model, of which the saturation effect is one of the most serious. In fact, due to the sensitivity difference of the three color channels, and fuzzy exposure controls, pixel saturation can happen incoherently in each of the color channels. The separate channel restoration near those saturated areas can result in over-amplification of that color component alone, thus creating artificial color mismatch and false coloring near those regions. To avoid this, we propose a novel mechanism that smoothly regulates the restoration process near saturated regions. The saturation control is integrated in the iterative solution of equation (19). The idea is to spatially adapt the update parameter  $\mu_i$  so as to limit the restoration effect near saturated areas. The adaptive update parameter is given as follows:

$$\mu_{i,adap}(m, n) = \beta_{sat}(m, n)\mu_i, \quad (20)$$

where  $\mu_i$  is the global step-size as discussed earlier, and  $\beta_{sat}$  is the local saturation control that modulates the step size.  $\beta_{sat}$  is obtained using the following algorithm:

- for each color channel image  $z_i$ ,  $i = \{1 \dots 4\}$ ,
- consider the values of the window ( $w \times w$ ) surrounding the pixel location  $z_i(m, n)$ ,
- count the number of saturated pixels  $S_i(m, n)$  in that window,



**Figure 7.** (a) Test image taken with a Nokia-6600 camera phone and reconstructed with the default processing chain. (b) Final image processed with the proposed deblurring of the raw data after 4 iterations, and reconstructed with the same chain.

- then the saturation control parameter is given by the following equation:

$$\beta_{sat}(m, n) = \max\{0, (w^2 - \sum_{i=1}^4 S_i(m, n))/w^2\}.$$

$\beta_{sat}$  varies between 0 and 1 depending on the number of saturated pixels in any of the color channels. Fig. 6 shows the effect of the proposed modification to avoid false coloring in the restored images. It can be seen from the examples that the proposed control procedure effectively suppresses the color mismatch near saturated areas.

#### 4.4. Image reconstruction chain

It is important to remind that this paper discusses the restoration of each of the color components as the first spatial filtering operation of the image reconstruction chain. So, for example, the overall resulting imaging chain can contain the following cascaded operations:

- Deblurring of color components (*proposed*)
- Pedestal noise removal
- Automatic White Balance
- Color Filter Array Interpolation
- Color gamut conversion
- Geometrical correction and vignetting elimination
- Noise reduction (optional)
- Sharpening (optional)

It is evident that the final image quality depends on the effective and optimized use of all these operations in the reconstruction chain. Typically, the most effective implementations of these algorithms are non-linear. As discussed earlier, the use of restoration as the first operation in the reconstruction chain ensures the best fidelity to the assumed linear model. The following algorithms, especially the color filter interpolation (CFAI) and the noise reduction algorithms, can act as additional regularization steps to prevent over-amplification due to excessive restoration.

Fig. 7 shows the final result that is obtained when we applied the proposed multichannel restoration algorithm in the reconstruction chain of a real camera system. The processing was carried out on the raw pictures captured

with Nokia 6600 camera-phone. As it can be seen from the images, there is an evident improvement in detail resolution and in color contrast. We have also tested with a large set of real scene images, and the visual quality of the obtained images with the proposed deblurring technique were consistently better than the images obtained with the default reconstruction chain.

## 5. CONCLUSION

In this paper, we have presented an integrated approach towards the reduction of optical blur into the camera image reconstruction chain. We have implemented a iterative Landweber algorithm together with adaptive de-noising technique, which uses the estimated PSF that characterizes the optical blurring for each color component. To avoid false coloring due to independent component filtering in RGB space, we have integrated a novel saturation control mechanism that smoothly attenuates the iterative restoration near saturated regions. Experimental results have shown that multi-channel image restoration effectively attenuates the blurring due to camera optics. The results show the potential of considering image deblurring, and, in general, formal restoration techniques as an integral part of imaging chains.

## REFERENCES

1. M. Banham and A. Katsaggelos, "Digital image restoration", *IEEE Signal Processing Magazine*, vol. 14, pp. 24-41, Mar. 1997.
2. M. Bertero and P. Boccacci, *Inverse Problems in Imaging*, IOP Publishing, pp. 138, 1998.
3. V. Katkovnik, K. Egiazarian and J. Astola, "A spatially adaptive nonparametric image deblurring", *IEEE Transactions on Image Processing* (In print).
4. L. Liang, Y. Xu, "Adaptive Landweber method to deblur images", *IEEE Signal Processing Letters*, vol. 10, no 5, pp. 129-132, 2003.
5. D. Biggs, M. Andrews, "Iterative blind deconvolution of extended objects", *International Conference on Image Processing, IEEE Proceedings*, vol. 2, pp. 454-457, Oct. 1997.
6. S. Lee, N. IK and J. Park, "Directional regularization for constrained iterative image restoration", *Electronic Letters*, vol. 39, Nov. 2003.
7. K. May, T. Stathaki and A. Katsaggelos, "Spatially adaptive intensity bounds for image restoration", *Eurasip Journal on Applied Signal Processing*, vol. 12, pp. 1167-1180, Dec. 2003.
8. V. Katkovnik, "A new method for varying adaptive bandwidth selection", *IEEE Trans. on Signal Proc.*, vol. 47, no. 9, pp. 2567-2571, 1999.
9. V. Katkovnik, K. Egiazarian, and J. Astola, "Adaptive window size image de-noising based on intersection of confidence intervals (ICI) rule". *J. of Math. Imaging and Vision*, vol. 16, N.3, pp. 223-235, 2002.
10. R. Molina, J. Mateos, A.K. Katsaggelos, and M. Vega, "A general multichannel image restoration method using compound models" *IEEE International Conference on Pattern Recognition (ICPR2002)*, vol. 3, pp. 835-838, 2002.
11. A. K. Katsaggelos and J. K. Paik, "Iterative color image restoration algorithms," *Proc. 1988 Int. Conf. Acoust., Speech, Signal Processing*, pp. 1028-1031, Apr. 1988.
12. M. Tekalp and G. Pavlovic, "Space-variant and color image restoration using Kalman filtering", *IEEE Symposium on Circuits and Systems*, vol. 1, pp. 8-11, 1989.
13. W. Na J. Paik and C. Lee, "An image restoration system for a single-CCD color camcorder", *IEEE Transactions On Consumer Electronics*, vol. 41, pp. 563-572, Aug. 1995.
14. E. Hecht, *Optics (4th edition)*, Addison Wesley, 2002.
15. O. Kalevo and H. Rantanen, "Sharpening methods for images captured through Bayer matrix", *Sensors, Cameras, and Applications for Digital Photography V, IS&T-SPIE's Electronic Imaging Science and Technology conference*, Jan. 2003.
16. M. Jiang. G. Wang, "Convergence studies on iterative algorithms for image reconstruction", *IEEE Transactions on Medical Imaging*, vol. 22, no. 5, pp. 569-579, 2003.
17. M. Figueiredo, R. Nowak, "An EM algorithm for wavelet-based image restoration", *IEEE Transactions on Image Processing*, vol. 12, issue 8, pp. 906 - 916, Aug. 2003.
18. <http://www.vision.caltech.edu/bouguetj/calibdoc/>